

Original Article

Exposure to *Pfaffia glomerata* causes oxidative stress and triggers hepatic changes

Exposição a *Pfaffia glomerata* causa estresse oxidativo e desencadeia alterações hepáticas

F. C. R. Dias^{a,b} , M. C. Cupertino^{c,d} , P. G. Silva^c , E. L. Oliveira^d , L. C. M. Ladeira^d , S. L. P. Matta^d , W. C. Otonif 
and M. L. M. Gomes^{a*} 

^aUniversidade Federal do Triângulo Mineiro – UFTM, Departamento de Biologia Estrutural, Uberaba, MG, Brasil

^bUniversidade Federal Rural de Pernambuco – UFRPE, Departamento de Veterinária, Recife, PE, Brasil

^cUniversidade Federal de Viçosa – UFV, Departamento de Medicina e Nutrição, Laboratório de Métodos Epidemiológicos e Computacionais em Saúde, Viçosa, MG, Brasil

^dUniversidade Federal de Viçosa – UFV, Departamento de Biologia Geral, Viçosa, MG, Brasil

^eUniversidade Federal de Viçosa – UFV, Departamento de Biologia Animal, Viçosa, MG, Brasil

^fUniversidade Federal de Viçosa – UFV, Departamento de Biologia Vegetal, Viçosa, MG, Brasil

Abstract

Medicinal plant species are genetically engineered to obtain higher production of biomass and specific secondary metabolites, which can be used in the pharmaceutical industry. The aim of the present study was to evaluate the effect of *Pfaffia glomerata* (Spreng.) Pedersen tetraploid hydroalcoholic extract on the liver of adult Swiss mice. The extract was prepared from the plant roots and given to the animals by gavage, for 42 days. The experimental groups were treated with water (control), *Pfaffia glomerata* tetraploid hydroalcoholic extract (100, 200 and 400 mg/kg) and *Pfaffia glomerata* tetraploid hydroalcoholic extract discontinuously (200 mg/kg). The last group received the extract every 3 days, for 42 days. The oxidative status, mineral dynamics, and cell viability were analysed. The liver weight and the number of viable hepatocytes were reduced, despite the increased cell's number. Increased levels of malondialdehyde and nitric oxide, and changes in iron, copper, zinc, potassium, manganese and sodium levels were observed. aspartate aminotransferase levels were increased while alanine aminotransferase levels were decreased due to BGEt intake. Our results showed that BGEt induced alterations of oxidative stress biomarkers leading to liver injury, which was associated with a reduction in the number of hepatocytes.

Keywords: toxicology, morphometry, hepatocyte, liver, phytotherapy.

Resumo

Espécies de plantas medicinais são geneticamente modificadas para obter maior produção de biomassa e metabólitos secundários específicos, que podem ser utilizados na indústria farmacêutica. O objetivo do presente estudo foi avaliar o efeito do extrato hidroalcoólico tetraploide de *Pfaffia glomerata* no fígado de camundongos suíços adultos. O extrato foi preparado a partir das raízes das plantas e administrado aos animais por gavagem, por 42 dias. Os grupos experimentais foram tratados com água (controle), extrato hidroalcoólico de *Pfaffia glomerata* tetraploide (100, 200 e 400 mg/kg) e extrato hidroalcoólico de *Pfaffia glomerata* tetraploide de forma descontínua (200 mg/kg). O último grupo recebeu o extrato a cada 3 dias, durante 42 dias. O estado oxidativo, a dinâmica mineral e a viabilidade celular foram analisados. O peso do fígado e o número de hepatócitos foram reduzidos, apesar do aumento do número de células. Observou-se aumento dos níveis de malondialdeído e óxido nítrico e alterações nos níveis de Ferro, Cobre, Zinco, potássio, Magnésio e sódio. Os níveis de aspartato aminotransferase aumentaram, enquanto os níveis de alanina aminotransferase diminuíram devido à ingestão do extrato. Nossos resultados mostraram que BGEt induziu alterações de biomarcadores de estresse oxidativo levando a lesão hepática, que foi associada a uma redução no número de hepatócitos.

Palavras-chave: toxicologia, morfometria, hepatócito, fígado, fitoterapia.

1. Introduction

An important number of plant species have been manipulated to obtain polyploid plants that produce higher amounts of biomass and specific secondary metabolites (Dhooghe et al., 2011; Caruso et al., 2013). Tetraploidy has been

linked to increased photoautotrophic potential, and higher production of the phytoecdisteroid 20-hydroxyecdisonone (20E) in the Brazilian ginseng (*Paffia glomerata* Spreng. Pedersen, Family Amaranthaceae) (Vigo et al., 2004).

*e-mail: marcos.gomes@uftm.edu.br

Received: January 26, 2023 – Accepted: May 16, 2023



This is an Open Access article distributed under the terms of the Creative Commons Attribution License, which permits unrestricted use, distribution, and reproduction in any medium, provided the original work is properly cited.

20E is considered the main active compound responsible for the adaptogenic and aphrodisiac properties of *P. glomerata* (Corrêa et al., 2016), along with providing relief from mental and physical stress (Carulo, 2012). However, 20E has been associated with increased levels of reactive oxygen species (ROS) negatively impacting male fertility (Dias et al., 2019).

Pharmacokinetic and pharmacodynamic studies are essential to establish the medicinal efficacy and toxicological safety of plant based compounds. This is important at a systemic level especially in the liver as the main site of nutrient metabolism and excretion of residual products. The liver is the main target of ROS since it controls the flow of substances absorbed by the digestive tract into the systemic circulatory system (Sánchez-Valle et al., 2012). Hepatocytes are more resistant to oxidative stress, however, Kupffer cells, stellate cells, and endothelial cells are more sensitive to ROS. When subjected to oxidative stress, Kupffer cells secrete tumor necrosis factor- α , which promotes inflammatory processes and apoptosis with consequent collagen synthesis and fibrosis of the organ (Li et al., 2015).

Despite its widespread application in traditional medicine, it is unclear whether the long-term intake of the hydroalcoholic extract of *P. glomerata* tetraploid accession (BGEt), rich in 20-hydroxyecdysone, induce pathological changes in liver tissue. To that end, animals ingested low (100 mg/kg) and high concentrations (200 and 400 mg/kg) of *P. glomerata* for 42 days. We focused on verifying whether the BGEt extract induces changes in biomarkers of oxidative stress leading to liver damage through histopathological, functional and oxidative parameters of the liver parenchyma.

2. Material and Methods

2.1. Extract preparation

Specimens of tetraploid *P. glomerata* (accession number 28) were obtained from the gene bank of the Plant Tissue Culture Laboratory, Federal University of Viçosa (UFV), Brazil. Samples were dried in an oven (55°C) and ground using a knife mill (SL32, Solab); the voucher specimen was deposited at the VIC Herbarium, Viçosa, Brazil (Code number VIC- 53,563).

The hydroalcoholic extract of tetraploid *P. glomerata* (BGEt) was obtained from 700g of roots, crushed for 48h with ethanol (95%), and percolated with the same solvent. After exhaustive extraction, the extract was evaporated under reduced pressure and lyophilized (VirTis BenchTop K lyophilizer) for complete solvent removal; a yield of 9.0% was attained.

2.2. Chromatographic profile of the extracts and quantification of the major compound in HPLC

The chromatographic profile, or fingerprint, was determined using HPLC with Shimadzu Prominence diode array detector (DAD) (LC - 20 AD pump, SPD - M 20 A detector, CTO - 20 A oven, LabSolutions software). The same sample used for phytochemical profile was used for chromatographic profile. The ethyl alcohol was removed using a rotary evaporator, and the samples were resuspended in methyl alcohol, HPLC purity.

The separations were performed into HPLC system by the auto sample injector. The column used in the elutions (Shimpack®, 15cm by 4.6mm) was reverse-phase (C-18), maintained at 30°C. The separation was made in a gradient system, using as mobile phase a mixture of methanol: water. In time from 0 to 5 min, methanol: water concentration ranged from 10:90 (v/v) to 70:30 (v/v). In time from 5 to 12 min, the concentration methanol: water remained at 70:30 (v/v), and at the time 12 to 15 min, the concentration of methanol: water ranged from 70:30 (v/v) to 100% of methanol. The detection wavelength was 245nm and flow rate of 1 mL/min, getting a run of 15min. The conditions were previously tested and optimized. The sample injection volume was 20 μ L.

The major compound quantification was made with a standard curve of 20-hydroxyecdysone (99% 20E purity; Sigma Chem. Co. USA). The chromatographic run presented the same conditions mentioned above, but in different concentrations (0.0024, 0.060, 0.12, 0.18, 0.23 and 0.29 mg/ml). Afterwards, a linear graph was generated, allowing us to obtain the equation of the curve used to calculate the concentration of the major compound.

2.3. Animals

All experimental procedures were approved by the UFV Ethics Committee on Animal Use (Protocol 044/2015). Male Swiss mice (n = 30; 55 days of age, 33.0 \pm 3.0 g) were housed under controlled temperature (22°C), humidity (60%–70%), and photoperiod (12h light/dark). Food and drinking water were provided *ad libitum*.

The animals were randomly divided into five groups (n = 6 animals/group): control (water), BGEt 100, 200, and 400 mg/kg (administered daily), and BGEt discontinuously (BGEtD) 200 mg/kg (administered every 3 days). All treatments were provided by oral gavage for 42 days. The extract was resuspended in water (0.5 mL), regardless of the concentration used. BGEt concentrations were chosen based on our previous results (Dias et al., 2019; Matta et al., 2020).

2.4. Sample collection

The animals were weighed and euthanized by deep anesthesia (i.p., thiopental, 30 mg/kg). Blood was harvested from the left ventricle via cardiac puncture. The liver was removed, weighed, and sectioned into three fragments for histopathological analysis. The first fragment was frozen in liquid nitrogen and stored at -80 °C for analysis of the oxidative status. The second fragment was immersed in Karnovsky fixative (Karnovsky, 1965), and the third fragment was immersed in a 30% KOH solution for 24 h for subsequent glycogen quantification. A small portion of frozen liver was used to assess tissue water content. The tissue was dried at 60°C for 96h to obtain a constant dry weight. The water content (mL/g) was calculated as the difference between the wet and dry liver weights.

2.5. Biochemical analysis

The blood of 6 animals was centrifuged at 4600 rpm for 20 min at 4°C. Serum was collected to evaluate aspartate aminotransferase (AST) and alanine transaminase (ALT).

Analyses were performed using biochemical kits (Bioclin Laboratories) suitable for the BS-200E chemical analyzer (Bioclin Laboratories, Brazil).

2.6. Liver oxidative stress markers

The frozen tissue of 6 animals was homogenized in potassium phosphate buffer (pH 7.4, 0.2M) containing 1M EDTA, and centrifuged at $13,800 \times g$ at 4°C for 10 min. The supernatant was employed to determine the concentration of superoxide dismutase (SOD), catalase (CAT), and glutathione S-transferase (GST). Nitric oxide (NO), malondialdehyde (MDA), and total protein content were also quantified. Values were normalized to total protein levels in the supernatant. All enzymatic activities were determined in duplicate using a spectrophotometer (UV-Mini 1240; Shimadzu) or an ELISA reader (Thermo Scientific).

2.7. Mineral content

The proportions of zinc (Zn), selenium (Se), copper (Cu), iron (Fe), and manganese (Mn) in the hepatic tissue of 6 animals were evaluated by X-ray dispersive energy spectroscopy (Ladeira et al., 2019). Briefly, liver fragments were dried at 60°C for 96h, coated with evaporated carbon (Quorum Q150 T), and analyzed using a scanning electron microscope (LEO 1430VP; Carl Zeiss) with a X-ray detector system (Tracor TN5502). The analysis was performed at $100\times$ magnification using an acceleration voltage of 20 kV and a working distance of 10 mm.

2.8. Body and liver biometry

The animals were weighed at the beginning and end of the experiment to determine any weight variations. To calculate the total volume of the organ, the liver of each animal was weighed and placed in a graded beaker containing 20mL of water. Based on the displacement of water inside the beaker, the volume of the organ was calculated and its density was derived as $d = m/v$. The relative weight of the liver (or hepatic somatic index, HSI) was calculated as $\text{HSI} (\%) = \text{liver weight} / \text{body weight} \times 100$ (Carvalho et al., 2022).

2.9. Histology

After fixation, liver fragments of 6 animals were dehydrated in ethanol and embedded in glycolmethacrylate resin (Historesin®; Leica). Semi-serial sections (1 and $3\mu\text{m}$ in thickness) were made at a distance of $40\mu\text{m}$ between sections. The $3\mu\text{m}$ -thick sections were stained with toluidine blue/sodium borate (1%) for morphometric and stereological analysis. Periodic acid-Schiff (PAS) was used to stain glycogen. Hematoxylin and eosin staining was used for histopathological analysis.

2.10. Proportion of liver components

To determine the proportions of the hepatic components, an orthogonal grid (266 intersections) was placed over the visual field of digital images taken randomly at $200\times$ magnification. Ten fields were analyzed per animal.

The cytoplasm and nucleus of hepatocytes, binucleated hepatocytes, blood vessels, sinusoid capillaries, lipid droplets, macrophages, and inflammatory infiltrates were counted. The volumetric proportion (Vv) of each component was calculated using the equation $Vv (\%) = PP / PT \times 100$ (PP= number of points pertaining to the structure of interest, and PT= total number of intersections (Carvalho et al., 2022).

2.11. Hepatocyte morphometry and stereology

The diameter of 30 hepatocyte nuclei was measured for each animal. The nuclear volume (NV, μm^3), cytoplasmic volume (CV, μm^3), and volume of each hepatocyte (HV, μm^3), were calculated according to the following formulae: $NV = 4/3 \pi R^3$ (R = nucleus radius), $CV = \% \text{ of cytoplasm} \times NV / \% \text{ of nuclei}$, and $HV = NV + CV$. The volume of hepatocytes in the liver (HV liver) was calculated using the formula: $HV \text{ liver} = \text{hepatocyte volume} \times \text{liver volume} / 100$. The total number of hepatocytes in the liver (HN) was calculated as $HN = HV \text{ liver} / HV$.

2.12. Hepatic glycogen concentrations

Glycogen was extracted as described by Oliveira et al. (2017). Briefly, fresh liver samples (50 mg) were digested by heating (100°C) in 0.5 mL of 5N KOH for 60 min. Glycogen was purified and precipitated with 99% ethanol in boiling water and then centrifuged at $8000 \times g$ for 20 min. The obtained pellets were resuspended in 1mL distilled water and 3mL anthrone solution (50mg diluted in 50mL of 84% H_2SO_4) and incubated for 10 min at 100°C . Absorbance was read at 620 nm (PowerWave X).

2.13. Histopathology

For histopathological analysis, a 266-point orthogonal grid was placed on digital images of the liver parenchyma at $200\times$ magnification. Ten fields were analyzed per animal. All points coinciding with regions of congestion or steatosis were counted. The volumetric proportion (Vv) of each component was calculated using the equation $Vv (\%) = PP / PT \times 100$ (PP= number of points pertaining to the structure of interest, and PT= total number of intersections (Carvalho et al., 2022).

2.14. Statistics

Normality was tested using the Shapiro-Wilk test. Data were tested using ANOVA, followed by the Student-Newman-Keuls test. Pearson's correlation was used to evaluate the relationships among variables. All statistical analyses were performed using the software Statistica, and the results were reported as mean \pm standard deviation of the mean. The level of significance was set to 5%.

3. Results

3.1. Quantification of the major compound

The chromatographic conditions applied were adequate to obtain chromatograms that allowed the visualization of a larger peak in the extract.

The purity of the compound was determined showing the ideal wavelength for reading (246nm - Figure 1), thus allowing the identification of the main compound, known as 20-hydroxyecdysone (20E). Using the standard curve, the equation that quantified the main compound was obtained, allowing the establishment of the amount offered daily per animal (100 mg/kg = 14.99 mg/kg/day, 200 mg/kg = 29.97 mg/kg/day, 400 mg/kg = 60.44 mg/kg/day).

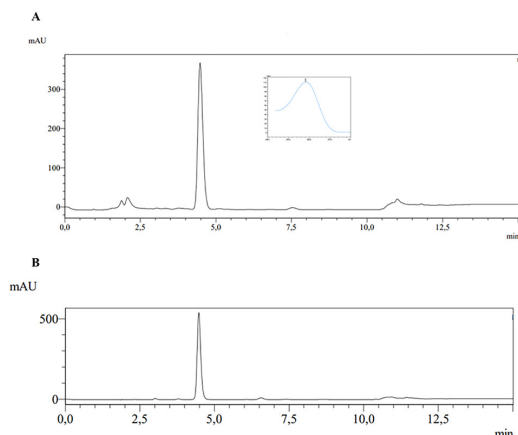


Figure 1. (A) Chromatogram of the hydroalcoholic root extract of *P. glomerata* tetraploid. In detail: peak of the major compound (20-hydroxyecdysone - 20E); (B) Chromatogram of the standard 20E. 246nm.

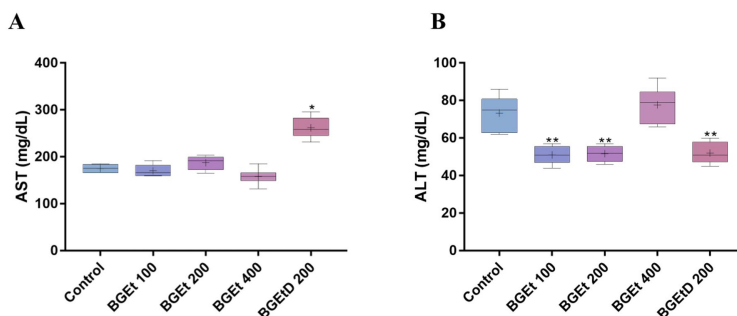


Figure 2. Serum parameters of hepatotoxicity after treatment with the hydroalcoholic extract of tetraploid *P. glomerata* (BGEt). (A) Aspartate aminotransferase (AST); (B) Alanine transaminase (ALT). Animals were treated with water (Control); daily doses of BGEt at 100, 200, and 400 mg/kg; or discontinuous doses of BGEtD at 200 mg/kg. *P < 0.05, **P < 0.01, ***P < 0.001 versus control.

Table 1. Body and liver weights, hepatic somatic index (HSI), and water content after BGEt intake.

Parameters	Control	BGEt 100	BGEt 200	BGEt 400	BGEtD 200
Body weight (g)	40.45±1.46 ^a	41.75±1.16 ^a	38.02±1.36 ^b	39.66±1.54 ^a	36.32±0.63 ^b
Body weight gain (g)	5.02±2.55 ^a	4.88±0.81 ^a	4.01±0.85 ^a	4.25±0.70 ^a	2.55±1.59 ^b
Liver weight (g)	2.20±0.03 ^a	2.24±0.23 ^a	1.92±0.04 ^b	2.08±0.14 ^a	1.50±0.15 ^b
HSI (%)	5.44±0.17 ^a	5.36±0.42 ^a	5.05±0.11 ^a	5.24±0.43 ^a	3.58±0.37 ^b
Liver volume (mL)	1.91±0.02 ^a	1.95±0.18 ^a	1.67±0.03 ^b	1.81±0.11 ^a	1.31±0.12 ^b
Liver density (g/mL)	1.15±0.01 ^a	1.12±0.06 ^a	0.96±0.10 ^c	1.04±0.11 ^a	1.50±0.13 ^b
Water content (mL/g)	33.85±2.27	30.84±4.73	36.65±1.43	37.47±1.28	36.36±2.44

Different superscripts (^{a,b,c}) indicate P < 0.05.

3.2. AST and ALT levels

AST levels were increased following intake of BGEtD 200 (Figure 2a); whereas ALT levels were decreased after intake of BGEt 100 and 200, as well as BGEtD 200 (Figure 2b).

3.3. Oxidative stress markers

NO levels were higher in all groups treated with BGEt (Figure 3a). The same was observed for MDA, except in the BGEt 200 group (Figure 3b). In contrast, total protein content was lower in all groups treated with BGEt (Figure 3c).

SOD activity was decreased in the BGEt 200 and 400 groups and increased in the BGEtD 200 group (Figure 3d). CAT activity was increased in the BGEt 100, 400, and BGEtD 200 groups (Figure 3e). GST levels were reduced in all treated groups (Figure 3f).

3.4. Mineral analysis

The proportion of Fe and Cu increased in all treated groups; whereas Na displayed the opposite behavior. K and Zn were higher in the BGEt 200 group; whereas Mg levels were lower in all treated groups, except in BGEtD 200 (Figure 4). Finally, the levels of Ca and Mn were not altered.

3.5. Body and liver biometry

At the beginning of the experiment, there was no statistical difference in body weight between animals; however, mice in the BGEtD 200 group failed to gain as much weight as others and the final weight in this group was lower (Table 1).

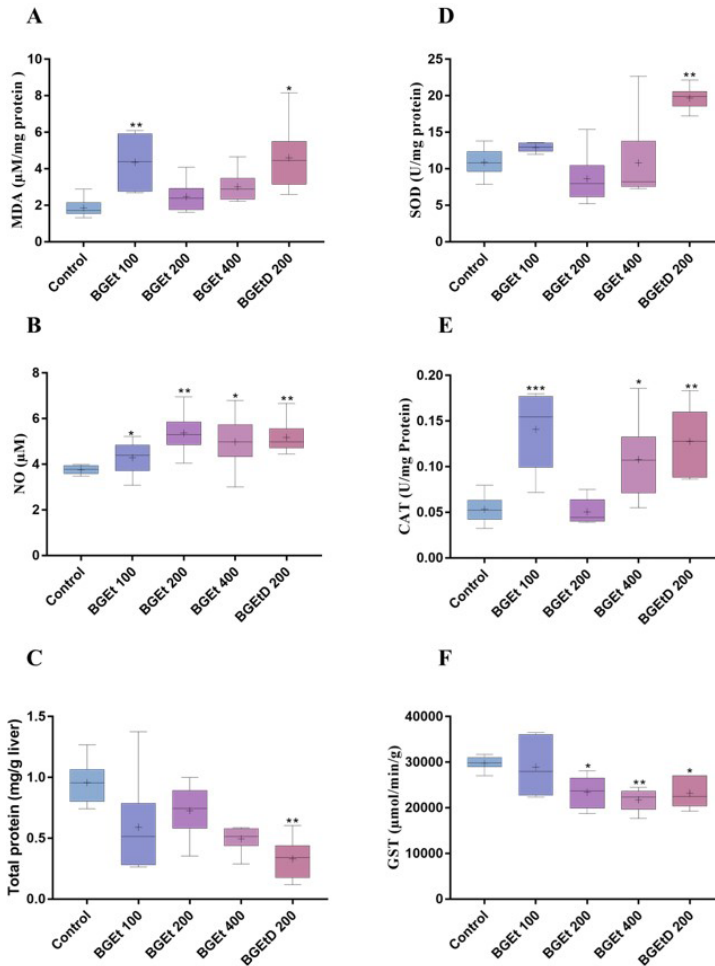


Figure 3. Oxidative/nitrosative stress markers. (A) Nitric oxide metabolites (NO²⁻ and NO³⁻); (B) Malondialdehyde (MDA); (C) Total protein; (D) Superoxide dismutase (SOD); (E) Catalase (CAT). (F) Glutathione S-transferase (GST). Animals were treated with water (Control); daily doses of BGEt at 100, 200, and 400 mg/kg; or discontinuous doses of BGEtD at 200 mg/kg. *P < 0.05, **P < 0.01, ***P < 0.001 versus control.

Liver weight and volume were lower in the BGEt 200 and BGEtD 200 groups, leading also to lower liver density in these individuals. HSI was lower in the BGEtD 200 group, whereas water content remained the same (Table 1).

3.6. Liver morphometry

Significantly fewer hepatocytes were observed in the liver parenchyma of animals from the BGEt 200 group. All groups appeared to have a smaller cytoplasm after BGEt intake (Figure 4), as confirmed by a higher cytoplasm-nucleus ratio in all BGEt-treated groups (Table 2). In addition, binucleated hepatocytes were significantly more abundant in the BGEt 100 and 200 groups (Figure 5).

Hepatocyte diameter and nuclear volume were higher in animals from the BGEtD 200 group. In comparison, the cytoplasmic volume was lower in the BGEt 100 and 200 groups, leading to an overall reduction in cell volume in these individuals (Table 2). Thus, the volume of hepatocytes was lower in both groups treated with the 200 mg/kg dose. The number of hepatocytes was higher in the BGEt 100, 200, and BGEtD 200 groups (Table 2).

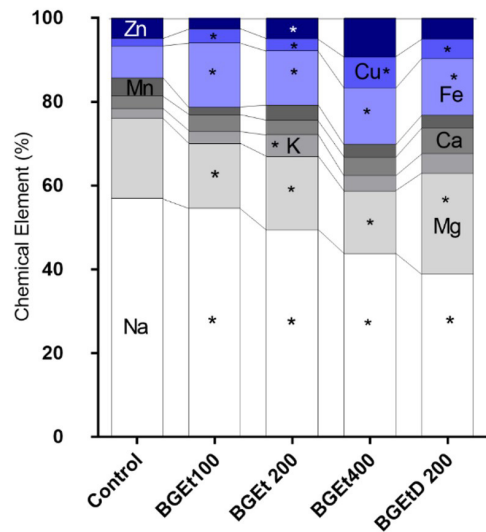


Figure 4. Proportions of minerals in hepatic tissue after BGEt intake. *P < 0.05.

Table 2. Hepatocyte morphometry and stereology.

Hepatocyte	Control	BGEt100	BGEt200	BGEt400	BGEtD200
Diameter (µm)	7.13±0.48 ^a	7.91±0.35 ^a	7.67±0.56 ^a	7.49±0.32 ^a	8.55±0.88 ^b
Nucleus Volume (µm ³)	191.57±40.05 ^a	259.76±33.85 ^a	238.96±51.92 ^a	220.92±27.87 ^a	336.14±105.80 ^b
Cytoplasm Volume (µm ³)	2574.38±504.47 ^a	1496.25±379.84 ^b	988.98±439.84 ^b	1726.03±460.47 ^a	2243.33±658.21 ^a
Cell Volume (µm ³)	2765.94±542.04 ^a	1756.01±407.09 ^b	1227.94±478.57 ^b	1946.95±476.53 ^a	2579.47±754.17 ^a
Cell Volume/Liver (µm ³)	0.016±0.0006 ^a	0.015±0.0045 ^a	0.012±0.0040 ^b	0.015±0.0027 ^a	0.007±0.0022 ^b
Cell number/liver (x10 ⁶)	11.29±1.77 ^a	17.79±3.40 ^b	20.50±4.27 ^b	16.78±3.45 ^b	30.4±0.92 ^b
NPR	0.56±0.08 ^a	3.26±1.05 ^b	3.44±0.56 ^b	1.87±0.90 ^b	2.36±0.82 ^b

NPR = nucleoplasmic ratio. Different superscripts (^{a,b}) indicate P < 0.05.

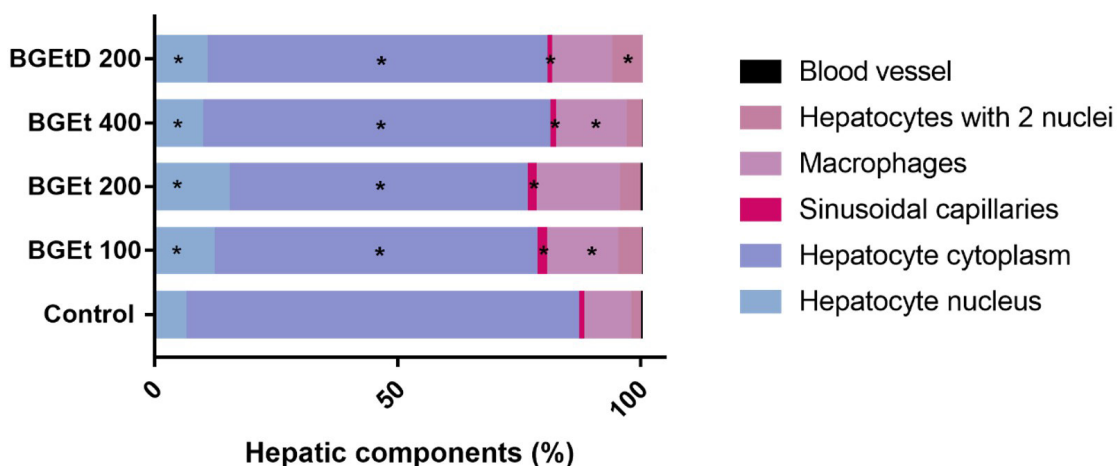


Figure 5. Proportions of the hepatic components. *P < 0.05.

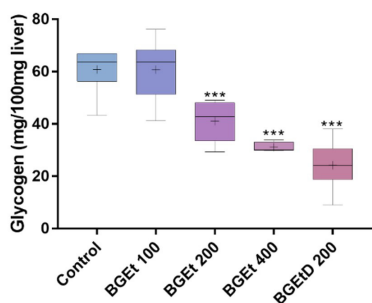


Figure 6. Glycogen amount per 100 mg of hepatic tissue. Animals were treated with water (Control); daily doses of BGEt at 100, 200, and 400 mg/kg; and discontinuous doses of BGEtD at 200 mg/kg. ***P < 0.001.

The proportion of sinusoids was higher in all groups treated with BGEt; whereas the proportion of blood vessels in the portal space remained unaltered (Figure 5). The proportion of Kupffer cells was increased in the BGEt 100 and BGEtD 200 groups (Figure 5).

3.7. Glycogen assay

The amount of glycogen was lower in BGEt 200, 400, and BGEtD 200 groups (Figure 6).

3.8. Histopathology

Vascular congestion was increased in the BGEt 100, 400, and BGEtD 200 groups. Steatosis was increased in the BGEt 200, 400, and BGEtD 200 groups (Figure 7).

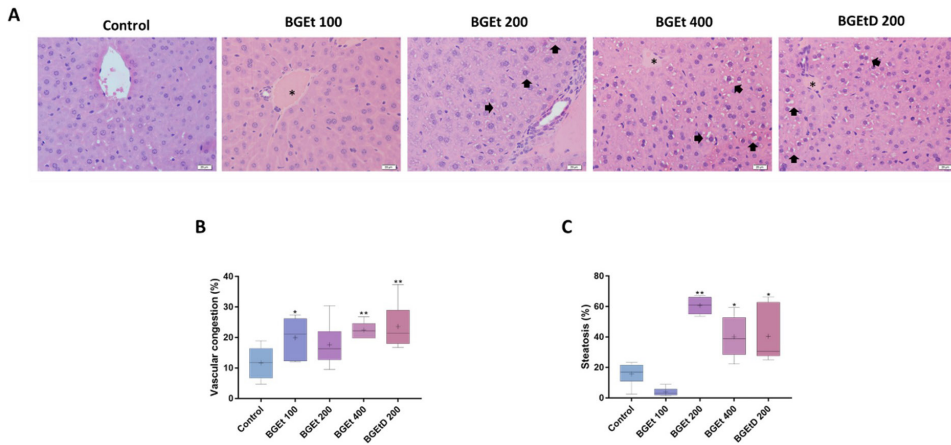


Figure 7. Histopathological analysis of liver tissue. (A) Photomicrographs of liver pathologies; (B) Vascular congestion (%); (C) Steatosis (%). Animals were treated with water (Control); daily doses of BGEt at 100, 200, and 400 mg/kg; and discontinuous doses of BGEtD at 200 mg/kg. In the images (*) - Congestion (arrow) - steatosis. In the graphics * $P < 0.05$, ** $P < 0.01$.

4. Discussion

The liver is the site of extensive metabolism and detoxification, which makes hepatocytes susceptible to injury (Lee et al., 2007). Usually start with a redox imbalance, whereby the cellular antioxidant machinery proves unable to neutralize ROS or reactive nitrogen species (RNS). This happens like decreased production of antioxidant enzymes or increased output of ROS/RNS. The resulting oxidative stress compromises lipids, proteins, and DNA (Therond, 2006), which may contribute to the onset and progression of liver damage (Li et al., 2015).

Hepatic homeostasis depends on the levels of minerals, important for the functioning of antioxidant enzymes, regulation of inflammatory responses, and transmission of cellular signals (Sun et al., 2012). SOD and CAT represent the first-line antioxidant defenses, and their balance plays an important role in the elimination of free radicals (Souza et al., 2018). Exposure to BGEt reduced SOD activity but increased CAT activity at all treatment doses, which likely resulted in an accumulation of superoxide anions that could not be detoxified to hydrogen peroxide and then neutralized by CAT.

Higher levels of Cu, Fe, and Mg were observed after BGEt intake, whereas Zn levels were increased only in the BGEt 200 group. Zn and Cu participate in redox regulation, as part of the Cu/Zn SOD isoform (Lee, 2018; Li and Yang, 2018; Yu et al., 2019). Zn is involved also in cell growth, development, and differentiation (Yu et al., 2019); whereas Cu acts as a cofactor for enzymes involved in energy metabolism, antioxidant defense, and Fe transport (Lee, 2018). Mg is widely distributed and highly compartmentalized; it is present in the nucleus, cytoplasm, mitochondria, and endoplasmic reticulum (Romani, 2007, 2008). It is involved in the synthesis and activation of many enzymes, the regulation of glucose and lipid metabolism in humans (Li et al., 2018), as well as DNA replication and repair, intermediate metabolism, ion transport, cell proliferation, and signal transduction (Larsson et al., 2005).

Thus, the changes observed in Mg levels after BGEt intake is possibly related to the damage observed in the hepatic tissue, and may eventually trigger liver diseases (Liu et al., 2019). Besides Cu, BGEt intake increased Fe level. The liver is responsible for regulating Fe metabolism, responding quickly and robustly to systemic changes. If Fe is abundant, the liver promotes its storage and protects other tissues from Fe-induced cellular damage (Yu et al., 2019; Kozeniecki et al., 2020). Cu acts directly on Fe metabolism. As previously mentioned, CAT activity increased after the daily ingestion of BGEt at 100 and 400 mg/kg or 200 mg/kg every 3 days. Increased Fe levels may lead to more ROS and lipid peroxidation being generated through the Fenton reaction (Casalino et al., 1997; Djukić-Čosić et al., 2008).

A reduction in Na levels, as observed here after BGEt ingestion, is common in cirrhosis and is related to impaired renal capacity to eliminate solute-free water (Gianotti and Cardenas, 2014). Another sign of liver damage is alterations in mitochondrial Ca levels, which promote ROS release and trigger the apoptotic cascade. However, Ca levels remained unchanged, meaning that liver cells regulating calcium signaling in different compartments (Oliva-Vilarnau et al., 2018).

ROS/RNS initiate lipid peroxidation, indiscriminately oxidizing biological membranes (Li et al., 2015). In the present study, MDA levels were higher in the BGEt 100, 400, and BGEtD 200 groups. NO levels increased in all experimental groups, as previously described for diploid *P. glomerata* (Dias et al., 2019). Despite participating in several cell signaling pathways, an exacerbated increase in NO tips the redox balance towards oxidative stress due to abundant RNS and may eventually lead to cell death (Sant'ana Dusse et al., 2003; Lee et al., 2005; Pasqualotto et al., 2006).

The reduced levels of GST following BGEt intake may indicate that this enzyme has been entirely used up. GST is responsible for cellular detoxification through conjugation to xenobiotic products and aldehydes generated during lipid peroxidation (Al-Bader et al., 1998). Additionally, GST may become inactivated by elevated levels of highly reactive free radicals (Regoli et al., 1998).

Oxidative stress and changes in mineral dynamics play a central role in the induction of cellular lesions by necrotic and/or apoptotic mechanisms, altering tissue morphology and physiology (Li et al., 2015). Overall, our findings indicate that BGEt ingestion induces hepatic damage and is associated with fewer viable hepatocytes in all treated groups. An increased number of hepatocytes were found to be either in the initial process of death or already dead, especially after being administered BGEt in a discontinuous way. Because 20E induces apoptosis by activating caspases 3 and 7, as well as pro-apoptotic genes, we believe that 20E triggered the intrinsic apoptotic pathways following mitochondria and DNA damage (Franco et al., 2009; Wang et al., 2016; Dias et al., 2019).

Damage caused is corroborated by increased serum levels of liver transaminases, which are traditional indicators of cellular lesions. Higher AST levels in the BGEtD 200 group implied liver damage, in line with the lower viability of hepatocytes and increased cell death in this group. This result may be associated with changes to the permeability of the cell membrane, with leakage of liver enzymes into the bloodstream (Reagan et al., 2012). Such scenario can be observed following exposure to different pollutants, including heavy metals, xenobiotics, carbon tetrachloride, and alcohol, which damage liver tissue and stimulate ROS production (Sreelatha et al., 2009). Plant species that are rich in alkaloids and flavonoids, such as the tomato *Solanum lycopersicum* L. (Buabeid et al., 2022) and *Bubulcus ibis coromandus* (Munir et al., 2022) may induce the increase in bilirubin, albumin, AST, ALT, ALP levels. In contrast, low ALT levels, as observed here, can be attributed to the action of plant polyphenols (Diab et al., 2020). ALT catalyzes the transformation of ketoacids such as pyruvate into amino acids such as alanine (Peltz-Sinvani et al., 2016). Low ALT levels are considered a biomarker of increased frailty and risk of mortality (Liu et al., 2014).

Our results evidence a relationship between markers of oxidative damage and morphological changes in the liver parenchyma (Liu et al., 2014). Histopathological analyses showed abundant lipid droplets within the hepatocyte cytoplasm, indicating steatosis. The lower amount of glycogen noticed after BGEt ingestion may be related to faster glucose consumption, as suggested by Oliveira (2012), describing the hypoglycemic activity of *P. glomerata*. The liver stores glycogen, converts galactose and fructose into glucose, is the site of gluconeogenesis, and mediates the formation of several important compounds from intermediates of carbohydrate metabolism. Hence, liver damage can lead to an imbalance of these functions.

The increased nucleus:cytoplasm ratio in hepatocytes following BGEt intake suggested some degree of cellular damage, reminiscent of that caused by ingestion of the herbicide paraquat (Novaes et al., 2012). The number of binucleated hepatocytes, which form when karyokinesis is not followed by cytokinesis, was higher in BGEt-treated animals. They represent the main cell type in the regenerating liver and are common after liver damage (Hammad et al., 2014). The higher number of hepatocyte nuclei indicates hepatic and non-cicatricial regenerative processes, which are characteristic of less intense liver lesions, and were corroborated here by the absence of fibrosis.

The response to hepatic tissue damage includes compensatory hyperplasia of the remaining parenchyma until the liver reaches its original weight (Parra et al., 1995).

Our study provides new information on hepatocyte morphometry. By applying a new histological method, it was possible to determine the absolute number of hepatocytes. This can be useful to discern whether increased liver weight is caused by a greater cell volume or simply more cells. In this regard, the nuclear diameter and volume of hepatocytes were increased in the BGEtD 200 group. Such pattern may result from more nuclear constituents in addition to DNA after tissue lesions. A more diffuse packaging of DNA in these cells may also contribute to nuclear enlargement (Jack et al., 1990), which may be related to increased protein synthesis (Christie and Le Page, 1961) or nucleolar activity (Deleener et al., 1987). The cytoplasmic and hepatocyte volumes were reduced in the BGEt 100 and 200 groups, which could be ascribed to inhibition of protein and glycogen synthesis, exocytosis, and bile flow (Kaiser, 1998). Such changes in cell volume led to a higher number of hepatocytes in the treated groups. Therefore, we speculate that the higher cell numbers observed in the liver of animals subjected to continuous treatment were due to a lower cell volume aimed at maintaining the weight and volume of the organ.

Hormones, oxidative stress, solute transport, and other stimuli alter the osmotic balance, whose effect on cell volume represents an intermediate step in a cascade affecting liver transport and metabolism. These effects are not limited to hepatocytes (Dunkelberg et al., 2001), as indicated by the increased proportion of Kupffer cells in BGEt-treated groups. This finding indicates increased secretion of regulatory and inflammatory factors during oxidative stress (Weng et al., 2018). Kupffer cells play a central role in hepatic and systemic responses to pathogens (Dixon et al., 2013) and remove toxic substances from the portal circulation (Simoniello et al., 2010).

5. Conclusions

The results show that exposure to BGEt triggers changes in mineral content, antioxidant enzymes (SOD, CAT, and GST), morphological and stereological parameters of the liver parenchyma. BGEt intake reduced body and liver weight, which stimulated cell division and increased the number of hepatocytes in the liver. Histopathological evaluation showed steatosis and lower glycogen levels in the hepatocytes cytoplasm. Finally, BGEt discontinuously administered induced substantial lipid peroxidation and oxidative stress, thus exacerbating liver damage being potentially toxic after 42 days of use.

Acknowledgements

The authors wish to thank Prof. T. Kamada (Universidade de Rio Verde, GO, Brazil), Dr. Roberto F. Vieira, and Dr. Rosa B. N. Alves (Embrapa/Cenargen, DF, Brazil) for providing the plant accession. We thank Dr. Kristhiano Chagas for growing the plants and for providing the root powder.

This study was funded by the Fundação de Amparo à Pesquisa do Estado de Minas Gerais (FAPEMIG) [grants numbers PRONEX-CAG-APQ-01036-09, CRA-APQ-01651-13, CRA-BPD-00046-14, and APQ-00772-19: to WCO]; and Fundação de Amparo à Ciência e Tecnologia de Pernambuco (FACEPE) [grant number BFP- 0002-5/21].

References

- AL-BADER, A., ABUL, H., HUSSAIN, T., AL-MOOSAWI, M., MATHEW, T.C. and DASHTI, H., 1998. Selenium and liver cirrhosis. *Molecular and Cellular Biochemistry*, vol. 185, no. 1-2, pp. 1-5. <http://dx.doi.org/10.1023/A:1006850514295>. PMID:9746205.
- BUABEID, M.A., ARAFA, E.S., RANI, T., AHMAD, F.U.D., AHMED, H., HASSAN, W. and MURTAZA, G., 2022. Effects of *Solanum lycopersicum* L. (tomato) against isoniazid and rifampicin induced hepatotoxicity in wistar albino rats. *Brazilian Journal of Biology = Revista Brasileira de Biologia*, vol. 84, pp. 84. PMID:35137848.
- CARULO, M.F., 2012. Use of SFC in extraction of adaptogens from Brazilian Plants. *American Journal of Analytical Chemistry*, vol. 3, no. 12, pp. 977-982. <http://dx.doi.org/10.4236/ajac.2012.312A129>.
- CARUSO, I., DAL PIAZ, F., MALAFRONTI, N., TOMMASI, N., AVERSANO, R., ZOTTELE, C.W., SCARANO, M.T. and CARPUTO, D., 2013. Impact of ploidy change on secondary metabolites and photochemical efficiency in *Solanum bulbocastanum*. *Natural Product Communications*, vol. 8, no. 10, pp. 1387-1392. <http://dx.doi.org/10.1177/1934578X1300801011>. PMID:24354181.
- CARVALHO, R.P.R., RIBEIRO, F.C.R., LIMA, T.I., ERVILHA, L.O.G., OLIVEIRA, E.L., FAUSTINO, A.O., LIMA, G.D.A. and MACHADO-NEVES, M., 2022. High doses of eugenol cause structural and functional damage to the rat liver. *Life Sciences*, vol. 304, pp. 120696. <http://dx.doi.org/10.1016/j.lfs.2022.120696>. PMID:35679916.
- CASALINO, E., SBLANO, C. and LANDRISCINA, C., 1997. Enzyme activity alteration by cadmium administration to rats: the possibility of iron involvement in lipid peroxidation. *Archives of Biochemistry and Biophysics*, vol. 346, no. 2, pp. 171-179. <http://dx.doi.org/10.1006/abbi.1997.0197>. PMID:9343363.
- CHRISTIE, G.S. and LE PAGE, R.N., 1961. Enlargement of liver cell nuclei: effect of dimethylnitrosamine on size and desoxyribosenucleic acid content. *Laboratory Investigation*, vol. 10, pp. 729-743. PMID:13693418.
- CORRÊA, J.P.O., VITAL, C.E., PINHEIRO, M.V.M., BATISTA, D.S., SALDANHA, C.W., DA CRUZ, A.C.F., NOTINI, M.M., FREITAS, D.M.S., DA MATTA, F.M. and OTONI, W.C., 2016. Induced polyploidization increases 20-hydroxyecdysone content, in vitro photoautotrophic growth, and ex vitro biomass accumulation in *Pfaffia glomerata* (Spreng.) Pedersen. *In Vitro Cellular & Developmental Biology. Plant*, vol. 52, no. 1, pp. 45-55. <http://dx.doi.org/10.1007/s11627-016-9746-9>.
- DELEENER, A., CASTELAIN, P., PREAT, V., DE GERLACHE, J., ALEXANDRE, H. and KIRSCH-VOLDERS, M., 1987. Changes in nucleolar transcriptional activity and nuclear DNA content during the first steps of rat hepatocarcinogenesis. *Carcinogenesis*, vol. 8, no. 2, pp. 195-201. <http://dx.doi.org/10.1093/carcin/8.2.195>. PMID:3802400.
- DHOOGHE, E., VAN LAERE, K., EECKHAUT, T., LEUS, L. and VAN HUYLENBROECK, J., 2011. Mitotic chromosome doubling of plant tissues in vitro. *Plant Cell, Tissue and Organ Culture*, vol. 104, no. 3, pp. 359-373. <http://dx.doi.org/10.1007/s11240-010-9786-5>.
- DIAB, K.A., FAHMY, M.A., HASSAN, E.M., HASSAN, Z.M., OMARA, E.A. and ABDEL-SAMIE, N.S., 2020. Inhibitory activity of black mulberry (*Morus nigra*) extract against testicular, liver and kidney toxicity induced by paracetamol in mice. *Molecular Biology Reports. Molecular Biology Reports*, vol. 47, no. 3, pp. 1733-1749. <http://dx.doi.org/10.1007/s11033-020-05265-1>. PMID:31983015.
- DIAS, F.C.R., MARTINS, A.L.P., DE MELO, F.C.S.A., CUPERTINO, M.C., GOMES, M.L.M., DE OLIVEIRA, J.M., DAMASCENO, E.M., SILVA, J., OTONI, W.C. and MATTA, S.L.P., 2019. Hydroalcoholic extract of *Pfaffia glomerata* alters the organization of the seminiferous tubules by modulating the oxidative state and the microstructural reorganization of the mice testes. *Journal of Ethnopharmacology*, vol. 233, pp. 179-189. <http://dx.doi.org/10.1016/j.jep.2018.12.047>. PMID:30605740.
- DIXON, L.J., BARNES, M., TANG, H., PRITCHARD, M.T., LAURA, E. and CLINIC, C., 2013. Kupffer Cells in the Liver. *Comprehensive Physiology*, vol. 3, no. 2, pp. 785-797. <http://dx.doi.org/10.1002/cphy.c120026>. PMID:23720329.
- DJKIĆ-ĆOSIĆ, D., ČURČIĆ JOVANOVIĆ, M., PLAMENAC BULAT, Z., NINKOVIĆ, M., MALIČEVIĆ, Ž. and MATOVIĆ, V., 2008. Relation between lipid peroxidation and iron concentration in mouse liver after acute and subacute cadmium intoxication. *Journal of Trace Elements in Medicine and Biology*, vol. 22, no. 1, pp. 66-72. <http://dx.doi.org/10.1016/j.jtemb.2007.09.024>. PMID:18319143.
- DUNKELBERG, J.C., FERANCHAK, A.P. and FITZ, J.G., 2001. Liver cell volume regulation: size matters. *Hepatology (Baltimore, Md.)*, vol. 33, no. 6, pp. 1349-1352. <http://dx.doi.org/10.1053/jhep.2001.24750>. PMID:11391521.
- FRANCO, R., SÁNCHEZ-OLEAB, R., REYES-REYES, E.M. and PANAYIOTIDIS, M.I., 2009. Environmental toxicity, oxidative stress and apoptosis: Ménage à Trois. *Mutation Research*, vol. 674, no. 1-2, pp. 3-22. <http://dx.doi.org/10.1016/j.mrgentox.2008.11.012>. PMID:19114126.
- GIANOTTI, R.J. and CARDENAS, A., 2014. Hyponatraemia and cirrhosis. *Gastroenterology Report*, vol. 2, no. 1, pp. 21-26. <http://dx.doi.org/10.1093/gastro/got037>. PMID:24760233.
- HAMMAD, S., FRIEBEL, A., BEGHER-TIBBE, B., AMNAH, O., VARTAK, A., HOEHME, S., EDLUND, K., VONRECKLINGHAUSEN, I., DRASDO, D. and HENGSTLER, J.G., 2014. Role of binucleated hepatocytes in hepatotoxicity and liver regeneration. *Naunyn-Schmiedeberg's Archives of Pharmacology*, vol. 387, pp. S46-S47.
- JACK, E.M., BENTLEY, P., BIERI, F., MUAKKASSAH-KELLY, S.F., STÄUBLI, W., SUTER, J., WAECHTER, F. and CRUZ-ORIVE, L.M., 1990. Increase in hepatocyte and nuclear volume and decrease in the population of binucleated cells in preneoplastic foci of rat liver: A stereological study using the nucleator method. *Hepatology (Baltimore, Md.)*, vol. 11, no. 2, pp. 286-297. <http://dx.doi.org/10.1002/hep.1840110220>. PMID:2307407.
- KAISER, S., 1998. Cell volume regulates liver phosphoenol pyruvate carboxykinase and fructose-1, 6-bisphosphatase genes. *The American Journal of Physiology*, vol. 274, no. 3, pp. 509-517. <http://dx.doi.org/10.1152/ajpgi.1998.274.3.G509>. PMID:9530152.
- KARNOVSKY, M.J., 1965. A formaldehyde-glutaraldehyde fixative of high osmolarity for use in electron microscopy. *The Journal of Cell Biology*, vol. 27, pp. 137-138.
- KOZENIECKI, M., LUDKE, R., KERNER, J. and PATTERSON, B., 2020. Micronutrients in Liver Disease: Roles, Risk Factors for Deficiency, and Recommendations for Supplementation. *Nutrition in Clinical Practice*, vol. 35, no. 1, pp. 50-62. <http://dx.doi.org/10.1002/ncp.10451>. PMID:31840874.

- LADEIRA, L.C.M., DOS SANTOS, E.C., VALENTE, G.E., SILVA, J., SANTOS, T.A. and MALDONADO, I.R.S.C., 2019. Could biological tissue preservation methods change chemical elements proportion measured by energy dispersive X-ray spectroscopy? *Biological Trace Element Research*, vol. 196, no. 1, pp. 168-172. <http://dx.doi.org/10.1007/s12011-019-01909-x>. PMID:31654256.
- LARSSON, S.C., BERGKVIST, L. and WOLK, A., 2005. Magnesium intake in relation to risk of colorectal cancer in women. *Journal of the American Medical Association*, vol. 293, no. 1, pp. 86-89. <http://dx.doi.org/10.1001/jama.293.1.86>. PMID:15632340.
- LEE, C.H., PARK, S.W., KIM, Y.S., KANG, S.S., KIM, J.A., LEE, S.H. and LEE, S.M., 2007. Protective mechanism of glycyrrhizin on acute liver injury induced by carbon tetrachloride in mice. *Biological & Pharmaceutical Bulletin*, vol. 30, no. 10, pp. 1898-1904. <http://dx.doi.org/10.1248/bpb.30.1898>. PMID:17917259.
- LEE, M.H., JANG, M.H., KIM, E.K., HAN, S.W., CHO, S.Y. and KIM, C.J.M., 2005. Nitric oxide induces apoptosis in mouse C2C12 myoblast cells. *Journal of Pharmacological Sciences*, vol. 97, no. 3, pp. 369-376. <http://dx.doi.org/10.1254/jphs.FPJ04017X>. PMID:15781989.
- LEE, R.S., 2018. Critical role of zinc as either an antioxidant or a prooxidant in cellular systems. *Oxidative Medicine and Cellular Longevity*, vol. 2018, pp. 1-11. <http://dx.doi.org/10.1155/2018/9156285>. PMID:29743987.
- LI, C., ZHAO, K., ZHANG, H., XIONG, F., WANG, K. and CHEN, B., 2018. Lead exposure reduces sperm quality and DNA integrity in mice. *Environmental Toxicology*, vol. 33, no. 5, pp. 594-602. <http://dx.doi.org/10.1002/tox.22545>. PMID:29446210.
- LI, L. and YANG, X., 2018. The essential element manganese, oxidative stress, and metabolic diseases: links and interactions. *Oxidative Medicine and Cellular Longevity*, vol. 2018, pp. 1-11. <http://dx.doi.org/10.1155/2018/7580707>. PMID:29849912.
- LI, S., TAN, H.Y., WANG, N., ZHANG, Z.J., LAO, L., WONG, C.W. and FENG, Y., 2015. The role of oxidative stress and antioxidants in liver diseases. *International Journal of Molecular Sciences*, vol. 16, no. 11, pp. 26087-26124. <http://dx.doi.org/10.3390/ijms161125942>. PMID:26540040.
- LIU, M., YANG, H. and MAO, Y., 2019. Magnesium and liver disease. *Annals of Translational Medicine*, vol. 7, no. 20, pp. 578-578. <http://dx.doi.org/10.21037/atm.2019.09.70>. PMID:31807559.
- LIU, Z., QUE, S., XU, J. and PENG, T., 2014. Alanine aminotransferase-old biomarker and new concept: A review. *International Journal of Medical Sciences*, vol. 11, no. 9, pp. 925-935. <http://dx.doi.org/10.7150/ijms.8951>. PMID:25013373.
- MATTA, A.P.F., LEITE, J.P.V., GOMES, M.L.M., MORAIS, D.B., CARVALHO, F.A.R., OTONI, W.C. and MATTA, S.L.P., 2020. Deleterious effects of *Pfaffia glomerata* (Spreng.) Pedersen hydroalcoholic extract on the seminiferous epithelium of adult Balb/c mice. *International Journal of Experimental Pathology*, vol. 101, no. 5, pp. 183-191. <http://dx.doi.org/10.1111/iep.12363>. PMID:32869402.
- MUNIR, M.A., ANJUM, K.M., JAVID, A., KHAN, N., JIANMING, C., NASEER, J., ANJUM, A., USMAN, S., SHAHZAD, M., HAFEEZ, S., HUSSAIN, T., SAEED, A., BADENI, A.H., MANSOOR, M.K. and HUSSAIN, I., 2022. Sublethal toxicity of carbofuran in cattle egret (*Bubulcus ibis coromandus*): hematological, biochemical, and histopathological alterations. *Brazilian Journal of Biology = Revista Brasileira de Biologia*, vol. 84, pp. 84. PMID:35019107.
- NOVAES, R.D., GONÇALVES, R.V., MARQUES, D.C.S., CUPERTINO, M.C., PELUZIO, M.C.G., LEITE, J.P.V. and MALDONADO, I.R.D.S., 2012. Effect of Bark Extract of *Bathysa cuspidata* on Hepatic Oxidative Damage and Blood Glucose Kinetics in Rats Exposed to Paraquat. *Toxicologic Pathology*, vol. 40, no. 1, pp. 62-70. <http://dx.doi.org/10.1177/0192623311425059>. PMID:22021167.
- OLIVA-VILARNAU, N., HANKEOVA, S., VORRINK, S.U., MKRRTCHIAN, S., ANDERSSON, E.R. and LAUSCHKE, V.M., 2018. Calcium signaling in liver injury and regeneration. *Frontiers in Medicine*, vol. 5, pp. 1-17. <http://dx.doi.org/10.3389/fmed.2018.00192>. PMID:30023358.
- OLIVEIRA, J.M., BRINATI, A., MIRANDA, L.D.L., MORAIS, D.B., ZANUNCIO, J.C., GONÇALVES, R.V., PELUZIO, M.C.G. and FREITAS, M.B., 2017. Exposure to the insecticide endosulfan induces liver morphology alterations and oxidative stress in fruit-eating bats (*Artibeus lituratus*). *International Journal of Experimental Pathology*, vol. 98, no. 1, pp. 17-25. <http://dx.doi.org/10.1111/iep.12223>. PMID:28449369.
- OLIVEIRA, W.C., 2012. *Reação de genótipos de Pfaffia glomerata (Spreng) Pedersen A Meloidogyne javanica e estudo morfo-anatômico da espécie hospedeira*. Brasília: Universidade Federal de Brasília, 95 p. Dissertação de Mestrado em Agronomia.
- PARRA, O.M., DE SOUSA E SILVA, R.A., DA SILVA, J.R., DA SILVA, J.R., HERNANDEZ-BLASQUEZ, F.J., PEDUTO, L., SAAD, W.A., and SAAD JUNIOR, W.A., 1995. Enhancement of liver size by stimulation of intact rat liver with exogenous hepatotrophic factors. *Sao Paulo Medical Journal*, vol. 113, pp. 941-947. <https://doi.org/10.1590/S1516-31801995000400004>. PMID: 8729872.
- PASQUALOTTO, F.F., PASQUALOTTO, E.B., UMEZU, F.M. and SALVADOR, M., 2006. Atividades da superóxido-dismutase e catalase no sêmen de homens férteis e inférteis. *Revista da AMRIGS*, vol. 50, pp. 130-134.
- PELTZ-SINVANI, N., KLEMPFNER, R., RAMATY, E., SELA, B.A., GOLDENBERG, I. and SEGAL, G., 2016. Low ALT levels independently associated with 22-year all-cause mortality among coronary heart disease patients. *Journal of General Internal Medicine*, vol. 31, no. 2, pp. 209-214. <http://dx.doi.org/10.1007/s11606-015-3480-6>. PMID:26245731.
- REAGAN, W.J., YANG, R.Z., PARK, S., GOLDSTEIN, R., BRESS, D. and GONG, D.W., 2012. Metabolic adaptive ALT isoenzyme response in livers of C57/BL6 mice treated with dexamethasone. *Toxicologic Pathology*, vol. 40, no. 8, pp. 1117-1127. <http://dx.doi.org/10.1177/0192623312447550>. PMID:22609950.
- REGOLI, F., NIGRO, M. and ORLANDO, E., 1998. Lysosomal and antioxidant responses to metals in the Antarctic scallop *Adamussium colbecki*. *Aquatic Toxicology (Amsterdam, Netherlands)*, vol. 40, no. 4, pp. 375-392. [http://dx.doi.org/10.1016/S0166-445X\(97\)00059-3](http://dx.doi.org/10.1016/S0166-445X(97)00059-3).
- ROMANI, A.M., 2007. Magnesium homeostasis in mammalian cells. *Frontiers in Bioscience*, vol. 12, no. 1, pp. 308-331. <http://dx.doi.org/10.2741/2066>. PMID:17127301.
- ROMANI, A.M., 2008. Magnesium homeostasis and alcohol consumption. *Magnesium Research*, vol. 21, no. 4, pp. 197-204. <http://dx.doi.org/10.1684/mrh.2008.0152>. PMID:19271417.
- SÁNCHEZ-VALLE, V.C., CHAVEZ-TAPIA, N., URIBE, M. and MENDEZ-SANCHEZ, N., 2012. Role of oxidative stress and molecular changes in liver fibrosis: a review. *Current Medicinal Chemistry*, vol. 19, no. 28, pp. 4850-4860. <http://dx.doi.org/10.2174/092986712803341520>. PMID:22709007.
- SANTANA DUSSE, L.M., VIEIRA, L.M. and CARVALHO, M.G., 2003. Revisão sobre óxido nítrico. *Jornal Brasileiro de Patologia e Medicina Laboratorial*, vol. 39, pp. 343-350.
- SIMONIELLO, P., FILOSA, S., RIGGIO, M., SCUDIERO, R., TAMMARO, S., TRINCHELLA, F. and MOTTA, C.M., 2010. Responses to cadmium intoxication in the liver of the wall lizard *Podarcis sicula*. *Comparative Biochemistry and Physiology. Toxicology & Pharmacology: CBP*, vol. 151, no. 2, pp. 194-203. <http://dx.doi.org/10.1016/j.cbpc.2009.10.005>. PMID:19861172.

- SOUZA, A.C.F., MARCHESI, S.C., LIMA, D.G.D.A. and MACHADO-NEVES, M., 2018. Effects of Arsenic Compounds on Microminerals Content and Antioxidant Enzyme Activities in Rat Liver. *Biological Trace Element Research*, vol. 183, no. 2, pp. 305-313. <http://dx.doi.org/10.1007/s12011-017-1147-3>. PMID:28879625.
- SREELATHA, S., PADMA, P.R. and UMADEVI, M., 2009. Protective effects of *Coriandrum sativum* extracts on carbon tetrachloride-induced hepatotoxicity in rats. *Food and Chemical Toxicology*, vol. 47, no. 4, pp. 702-708. <http://dx.doi.org/10.1016/j.fct.2008.12.022>. PMID:19146910.
- SUN, L., YU, Y., HUANG, T., AN, P., YU, D., YU, Z., LI, H., SHENG, H., CAI, L., XUE, J., JING, M., LI, Y., LIN, X. and WANG, F., 2012. Associations between ionomic profile and metabolic abnormalities in human population. *PLoS One*, vol. 7, no. 6, pp. e38845. <http://dx.doi.org/10.1371/journal.pone.0038845>. PMID:22719963.
- THEROND, P., 2006. Stress oxydant Dommages créés aux biomolécules. *Annales Pharmaceutiques Francaises*, vol. 64, pp. 383-389. [http://dx.doi.org/10.1016/S0003-4509\(06\)75333-0](http://dx.doi.org/10.1016/S0003-4509(06)75333-0). PMID:17119467.
- VIGO, C.L.S., NARITA, E. and MARQUES, L.C., 2004. Influências da variação sazonal e tipos de secagem nas características da droga vegetal - raízes de *Pfaffia glomerata* (Spreng.) Pedersen (Amaranthaceae). *Revista Brasileira de Farmacognosia*, vol. 14, no. 2, pp. 137-144. <http://dx.doi.org/10.1590/S0102-695X2004000200007>.
- WANG, D., PEI, X.Y., ZHAO, W.L. and ZHAO, X.F., 2016. Steroid hormone 20-hydroxyecdysone promotes higher calcium mobilization to induce apoptosis. *Cell Calcium*, vol. 60, no. 1, pp. 1-12. <http://dx.doi.org/10.1016/j.ceca.2016.05.003>. PMID:27209368.
- WENG, T.I., CHEN, H.J., LU, C.W., HO, Y.C., WU, J.L., LIU, S.H. and HSIAO, J.K., 2018. Exposure of macrophages to low-dose gadolinium-based contrast medium: impact on oxidative stress and cytokines production. *Contrast Media & Molecular Imaging*, vol. 2018, pp. 3535769. <http://dx.doi.org/10.1155/2018/3535769>. PMID:30627059.
- YU, L., LIOU, I.W., BIGGINS, S.W., YEH, M., JALIKIS, F., CHAN, L.N. and BURKHEAD, J., 2019. Copper deficiency in liver diseases: a case series and pathophysiological considerations. *Hepatology Communications*, vol. 3, no. 8, pp. 1159-1165. <http://dx.doi.org/10.1002/hep4.1393>. PMID:31388635.